J Mol Model (2013) 19:3165–3174
DOI 10.1007/s00894-013-1842-8

ORIGINAL PAPER

Key role of hydrazine to the interaction between oxaloacetic against phosphoenolpyruvic carboxykinase (PEPCK): ONIOM calculations

Pongthep Prajongtat · Darinee Sae-Tang Phromyothin · Supa Hannongbua

Received: 7 September 2012 / Accepted: 1 April 2013 / Published online: 27 April 2013

Abstract The interactions between oxaloacetic (OAA) and phosphoenolpyruvic carboxykinase (PEPCK) binding pocket in the presence and absence of hydrazine were carried out using quantum chemical calculations, based on the two-layered ONIOM (ONIOM2) approach. The complexes were partially optimized by ONIOM2 (B3LYP/6-31G(d):PM6) method while the interaction energies between OAA and individual residues surrounding the pocket were performed at the MP2/6-31G(d,p) level of theory. The calculated interaction energies (*INT*) indicated that Arg87, Gly237, Ser286, and Arg405 are key residues for binding to OAA with the *INT* values of −1.93, −2.06, −2.47, and −3.16 kcal mol^{-1}, respectively. The interactions are mainly due to the formation of hydrogen bonding interactions with OAA. Moreover, using ONIOM2 (B3LYP/6-31G(d):PM6) applied on the PEPCKHS complex, two proton transfers were observed; first, the proton was transferred from the carboxylic group of OAA to hydrazine while the second one was from Asp311 to Lys244. Such reactions cause the generation of binding strength of OAA to the pocket via electrostatic interaction. The orientations of Lys243, Lys244, His264, Asp311, Phe333, and Arg405 were greatly deviated after hydrazine incorporation. These indicate that hydrazine plays an important role in terms of not only changing the conformation of the binding pocket, but is also tightly bound to OAA resulting in its conformation change in the pocket. The understanding of such interaction can be useful for the design of hydrazine-based inhibitor for antichachexia agents.

Keywords Hydrazine · Interaction energy · ONIOM · Oxaloacetic · Phosphoenolpyruvic carboxykinase

Electronic supplementary material The online version of this article (doi:10.1007/s00894-013-1842-8) contains supplementary material, which is available to authorized users.

P. Prajongtat · S. Hannongbua (✉)
Department of Chemistry, Faculty of Science,
Kasetsart University, Chatuchak,
Bangkok, Thailand 10900
e-mail: fscisph@ku.ac.th

P. Prajongtat · S. Hannongbua
Center of Nanotechnology KU,
and NANOTEC Center of Excellence,
Kasetsart University, Chatuchak,
Bangkok, Thailand 10900

D. S.-T. Phromyothin
College of Nanotechnology,
King Mongkut's Institute of Technology Ladkrabang,
Chalongkrung Rd., Ladkrabang,
Bangkok 10520, Thailand

Introduction

Conventional methods for cancer treatment such as surgery, chemotherapy, and radiation therapy always damage the healthy cells. Therefore, the unconventional methods, e.g., hydrazine sulfate, green tea, 714-X, essiac, iscador, vitamins A, E, and C are frequently used in combination with the conventional therapeutic methods for cancer treatment [1, 2]. However, none of proper clinical evidence showing the valuable advantage of such compounds as drugs themselves for curing the cancer patients has been reported [2]. The true potential of unconventional treatments might be considered in terms of adjunctive and palliative care. Among the unconventional methods, hydrazine sulfate has attracted considerable attention as an antichachexia agent used in cancer patients, but not directly induced antitumor responses [3]. Such a compound has been first studied based on cell lines

and animal models by Gold [4–7]. The obtained results found that hydrazine sulfate can inhibit tumor growth and increase survival in rats with transplanted tumors [4] and also improve appetite and reduce weight loss in cancer patients [5, 6]. Two mechanisms of hydrazine sulfate explaining its potential for antichachexia properties were proposed elsewhere. In the first mechanism, hydrazine is a noncompetitive inhibitor of phosphoenolpyruvate carboxykinase (PEPCK) enzyme in the gluconeogenesis process by blocking the conversion of oxaloacetic to phosphoenolpyruvic through PEPCK inhibition [8–10]. Inhibition of gluconeogenesis process through PEPCK enzyme can interfere in the supply of nutrients to tumor, and consequently the tumor growth is reduced because cancer cells cannot use excessive glucose for their growing. The second mechanism, hydrazine sulfate inhibits tumor necrosis factor-alpha (TNF-α) activity [11]. TNF-α known as chachectin is a chemical produced by body white blood cells against the inflection and damage of tissues by microorganisms. The higher-than-normal levels of TNF-α in cancer patients can cause the requirement of much energy expenditure and muscle breakdown [12, 13].

Nevertheless, severe results of the use of hydrazine were also reported. For instance, Toth found that hydrazine significantly increased the incidence of lung tumors in Swiss mice [14]. Hainer et al. reported that the patients who were administered hydrazine sulfate were found to have fatal hepatorenal failure [15]. The use of hydrazine was also reported to be related to acute kidney injury and multiorgan failure, ultimately promoting death in patients [16]. Thus, hydrazine might be of considerable attraction as a prototype to therapeutical developments in the future. The hydrazine derivatives have been synthesized and applied for cancer treatment. 3-methylbenzyl-2-(6-methylpyridin-2-ylmethylene)hydrazine carbodithioate (6mpyS3M) and transition metals (Cu(II), Ni(II), Zn(II) and Cd(II)) were prepared and used as the effective active agents for treatment of breast cancer cell lines [17]. 1,2-Bis(methylsulfonyl)-1-(2-chloroethyl)-2-[[1-(4-nitrophenyl)ethoxy]carbonyl] hydrazine (KS119) [18] and 1,2-bis(methylsulfonyl)-1-methyl-2-[[1-(4-nitrophenyl)ethoxy]carbonyl]hydrazine (KS900) [19] were applied to cancerous tissues under oxygen deficiency conditions resulting in the resistance of tumor metastasis. The 2-(4-alkoxyphenyl) cyclopropyl hydrazide derivatives were synthesized. The derivatives with the isopentenyl and geranyl side-chains showed more effective apoptosis-resistant cancer properties than other compounds [20]. A series of *N*-mustard-quinoline conjugates having urea and hydrazinecarboxamide linkage were prepared for inhibiting human lymphoblastic leukemia and tumor growth; however, the compounds with hydrazinecarboxamide linkage demonstrated more cytotoxic than urea linkage [21]. Some compounds of pyrroloquinoxaline with hydrazine moiety derivatives acted as the promising cytotoxic agents in a panel of cancer cell lines in both in vitro and in vivo experiments [22]. 3-aryl-1-(4-tert-butylbenzyl)-1H-pyrazole-5-carbohydrazide hydrazone derivatives had the ability to inhibit the growth of A549 lung cancer cells [23].

Oxaloacetic acid (OAA), an intermediate in the gluconeogenesis pathway, is naturally synthesized inside the mitochondrial matrix. It was expected that the transportation of OAA in rat liver mitocondria might be occurred by the oxoglutarate carrier, which catalyzes the exchange between OAA and oxoglutarate [24]. OAA is produced by carboxylation of pyruvate in the presence of one molecule of ATP and a divalent metal ion, as shown in reaction (1) [25]. This reaction is catalyzed through pyruvate carboxylase in vertebrates, invertebrates, fungi, and certain bacteria. The formation of OAA from pyruvate allows the tricarboxylic acid cycle to fulfill the gluconeogenesis.

$$\text{Pyruvate} + HCO_3^- + \text{ATP} \xrightarrow{Me^{2+}} \text{OAA} + \text{ADP} + \text{Pi} \qquad (1)$$

OAA is transferred to the cytosol as malate [26] and further decarboxylated and simultaneously phosphorylated by PEPCK in the presence of a nucleoside triphosphate (ATP or GTP, depending on the enzyme source) to produce phosphoenolpyruvate (PEP), as presented in reaction (2) [27].

$$\text{OAA} + \text{ATP/GTP} \xrightarrow{Me^{2+}} \text{PEP} + \text{GDP} + CO_2 \qquad (2)$$

On the other hand, theoretical investigation has been successfully applied for biological systems to obtain more details about structural and energetic properties. To understand the role of hydrazine in the binding of OAA to PEPCK binding pocket, the ONIOM (our own *n*-layered integrated molecular orbital and molecular mechanics) method [28] were employed in this study. The ONIOM method has been a great success for large systems such as the enzyme-ligand interaction due to the compromise between accuracy and computational cost [29–38]. The ONIOM method reduces the computational effort by partitioning the model system into two or three layers which are treated with different levels of theory. The inner layer involving the important ligand/inhibitor and/or some key amino residues is treated with a high level of theory, e.g., ab initio calculation and density functional theory (DFT), whereas the rest of the system, outer layer, is treated with a low level of theory, e.g., the semi-empirical method and molecular mechanic (MM). In this work, the B3LYP/6-31G(d) method combined with PM3, PM3MM and PM6 semi-empirical methods was selected in ONIOM2 due to its successful applications in several enzyme-inhibitor interactions such as HIV-1 reverse transcriptase [30–34,

38], Acetylcholine esterase [29], Cyclooxyginase type II [35] and Dihydrofolate reductase [36]. In case of inhibitor consisting of aromatic system, the high level treated by the second-order Møller-Plesset perturbation theory (MP2) method is required to observe weak attractive interaction such as H-π or π-π interaction [38]. In addition, in the present work, the interaction energy calculations between individual residues and OAA were carried out using MP2 method for explaining the hydrogen bonding interactions existing in the investigated systems [32]. Thus, the main objective of this work is to understand the key role of hydrazine in blocking gluconeogenesis process through PEPCK enzyme by employing quantum chemical calculations based on ONIOM2 method. The understanding of the role of hydrazine inhibitor in PEPCK complex can be useful in the design of new specific hydrazine derivatives used for cancer related cachexia treatment.

Computational methods

System setup

The crystal structure of PEPCK complexed with OAA was obtained from protein data bank (code 2QF1) [39]. The surrounding 13 residues in the radius of about 7 Å centered at OAA, including Arg87, Gly236, Gly237, Lys243, Lys244, His264, Ser286, Ala287, Asp311, Phe333, Gly334, Arg405, and Phe485, were initially selected in this study. This radius is sufficient for including whole residues which interact with OAA through short- and long-range interactions. The schematic illustration of OAA bound to the PEPCK binding site is shown in Fig. 1a. The model was terminated at the N and C termini of the residues by an acetyl group (CH3CO-) and methyl amino group (−NHCH3), respectively. All heavy atoms were fixed and hydrogen atoms were added to generate the complete structure by using Sybyl7.2 program [40]. The added hydrogen atoms were optimized with heavy atoms fixing (HAF) and backbone atoms fixing (BBF) approaches using the PM3 and ONIOM2 (B3LYP/6-31G(d):PM3) methods. For the ONIOM2 calculations, only OAA (13 atoms) was treated with the high level of theory while the residues surrounding the pocket (308 atoms) were treated by PM3 semi-empirical calculations. All calculations were performed in gas phase using the Gaussian 09 program package [41].

Hydrazine docking

Since the X-ray structure of PEPCK complexed with hydrazine is not available, therefore, a hydrazine molecule was docked into the PEPCK structure (2QF1.pdb) using Autodock3 program [42]. A three-dimensional (3D) grid was created with the AutoGrid algorithm with 120x120x120 grid points. The affinity and electrostatic potential grids were calculated for each type of atom of hydrazine. The docking using Lamarckian genetic algorithm was applied. The maximum number of generations, energy evaluations, and docking runs were set to 27000, 250000, and 100, respectively. The other parameters were set as default. Atomic charges were taken as Kollman-all-atoms for PEPCK enzyme and Gasteiger-Hückel for the hydrazine [43]. The most stable structure with the lowest energy and largest population was selected for the further step.

ONIOM2 calculations

The effect of hydrazine in the binding of OAA to the PEPCK pocket was investigated based on the docked complex structure. The ONIOM2 models were composed of two layers; for the PEPCK complex including hydrazine (hereafter denoted as PEPCKHS), both OAA and hydrazine were considered as the inner layer (19 atoms) and treated with the B3LYP/6-31G(d) method while the residues surrounding OAA and hydrazine were expanded to include eight additional residues (Phe284, Pro285, Cys288, Gly289, Lys290, Thr291, Asn292, and Val335), resulting in 21 residues (Fig. 1b, 425 atoms) as the outer layer and calculated with the PM3 semi-empirical method. In the case of PEPCK complex not including hydrazine (hereafter denoted as PEPCKnoHS) the inner layer, only OAA (13 atoms), was treated with the B3LYP/6-31G(d) method while the outer layer was treated with similar manner to PEPCKHS. Moreover, we also examined the effect of the outer layer which was treated with different semi-empirical methods, i.e., PM3, PM3MM, and PM6, to the orientation of the ligand (OAA) in the pocket. The binding energies (BE^{ONIOM}) between OAA and the binding pocket were calculated as the following equations:

PEPCKnoHS:

$$BE^{\mathrm{ONIOM}} = E^{\mathrm{ONIOM}}_{\mathrm{complex}} - E^{\mathrm{semi-empirical}}_{\mathrm{pocket}} - E^{\mathrm{B3LYP}}_{\mathrm{OAA}} \quad (3)$$

PEPCKHS:

$$BE^{\mathrm{ONIOM}} = E^{\mathrm{ONIOM}}_{\mathrm{complex}} - E^{\mathrm{ONIOM}}_{\mathrm{pocket}} - E^{\mathrm{B3LYP}}_{\mathrm{OAA}}, \quad (4)$$

where $E^{\mathrm{ONIOM}}_{\mathrm{complex}}$ is the total energy of the complex calculated from the ONIOM2 method. $E^{\mathrm{semi-empirical}}_{\mathrm{pocket}}$ and $E^{\mathrm{ONIOM}}_{\mathrm{pocket}}$ are the total energies of the binding pocket obtained from the PM3 and ONIOM2 calculations, respectively. $E^{\mathrm{B3LYP}}_{\mathrm{OAA}}$ is the total

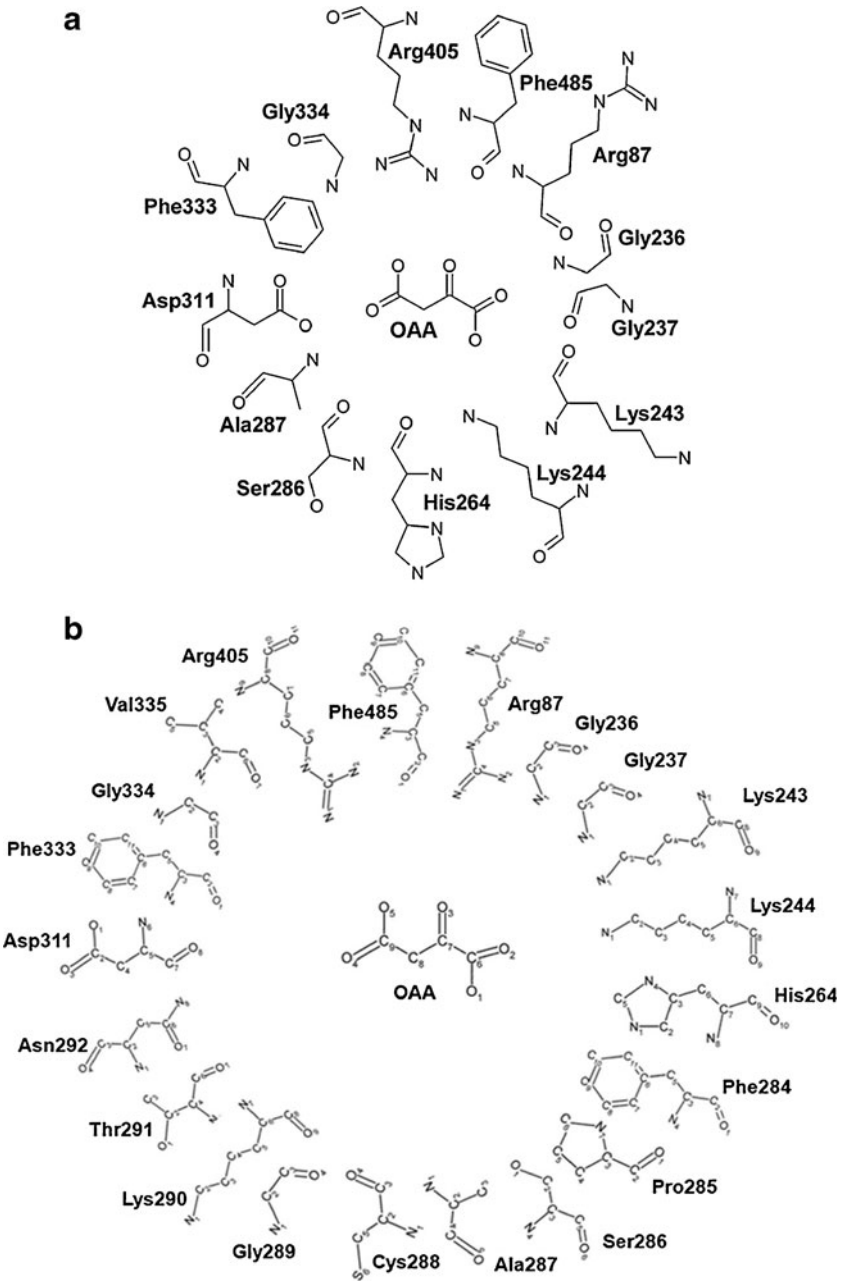

Fig. 1 Schematic illustration of oxaloacetic bound to PEPCK binding site **a** including 13 residues for method validation **b** including 21 residues for ONIOM2 calculations

energy of oxaloacetic calculated by the B3LYP/6-31G(d) level of theory. According to Eq. (4) the hydrazine molecule was included into the pocket when calculating the total energy of the pocket of PEPCKHS.

Interactions between oxaloacetic and individual residues

The interaction energies between OAA and the 21 individual residues (defined as X_i) surrounding the PEPCK binding pocket for both PEPCKnoHS and PEPCKHS complexes were performed using the MP2/6-31G(d,p) level of theory with the BSSE correction. The geometries of both systems were obtained from ONIOM2 (B3LYP/6-31G(d):PM6) optimization. The MP2 method precisely describing the polarization and dispersion is suitable for investigating the biological system involving the H-π and π-π interactions [24]. The effect of hydrazine inclusion to the binding of OAA and the pockets was then discussed. The interaction energy between OAA and X_i (INT_{OAA+Xi}) is defined as following:

$$INT_{OAA+Xi} = E_{OAA+Xi} - E_{OAA} - E_{Xi}, \quad (5)$$

where E_{OAA+xi}, E_{OAA}, and E_{Xi} are the energies of OAA bound to individual residues, isolated OAA, and individual residues, respectively.

Results and discussion

Comparison of structures and binding energies of HAF and BBF optimizations

In order to achieve the reliable geometries with the reasonable computational time the optimization of the PEPCK-OAA complex including OAA and 13 residues in the radius of about 7 Å centered at OAA with heavy atoms fixing (HAF) and backbone atoms fixing (BBF) were performed. In the HAF optimization, only OAA molecule and hydrogen atoms were relaxed while other heavy atoms were fixed at the X-ray position. For the BBF optimization, the side chain atoms of residues were also relaxed, whereas only backbone atoms of residues were fixed. The PM3 semi-empirical optimization was first taken into account. The calculated binding energies of OAA and the binding pocket with the HAF and BBF approaches are found to be −11.30 and −15.69 kcal mol^{-1}, respectively. These results indicate that the BBF optimization provides more stable geometry than that calculated from the HAF optimization due to significantly lower binding energy of about 4.39 kcal mol^{-1}.

The high accurate optimization method based on the ONIOM2 approach was then applied to this system. The superimposition of backbone atoms of the ONIOM2 optimized structures with HAF and BBF approximations are displayed in Fig. 2a. Comparison between the geometries with both approximations demonstrates a slight difference with the RMSD of 0.79 Å as a result of the relaxation of amino side chains and OAA during the BBF optimization procedure. Similarly to the whole PM3 calculations, the BBF binding energy (−10.89 kcal mol^{-1}) calculated from the ONIOM2 scheme is lower than that of the HAF value (−7.36 kcal mol^{-1}), which strongly confirms that the optimization with the BBF approach gives far more reasonable structure than the HAF approach. In addition, the BBF approach does not cost much additional effort compared to the HAF approach. Therefore, the BBF approach was chosen for further calculations.

Effect of hydrazine in the binding of oxaloacetic and binding pocket

We classified our investigated models into two systems, PEPCKHS and PEPCKnoHS. The model systems consist of hydrazine (for PEPCKHS)/no hydrazine (for PEPCKnoHS), OAA, and surrounding 21 residues including Arg87, Gly236, Gly237, Lys243, Lys244, His264, Phe284, Pro285, Ser286, Ala287, Cys288, Gly289, Lys290, Thr291, Asn292, Asp311, Phe333, Gly334, Val335, Arg405, Phe485. The variation of semi-empirical methods, PM3, PM3MM, and PM6, for the outer layer was studied by fixing the high level method at B3LYP/6-31G(d). The PEPCKnoHS complex was partially optimized using the ONIOM2 method with the BBF approach. The superimposition of backbone atoms of the X-ray, B3LYP/6-31G(d):PM3, B3LYP/6-31G(d):PM3MM, and B3LYP/6-31G(d):PM6 optimized structures is shown in Fig. 2b. It is clearly seen that the B3LYP/6-31G(d):PM3 structure is very similar to one calculated from the B3LYP/6-31G(d):PM3MM method, but slightly different

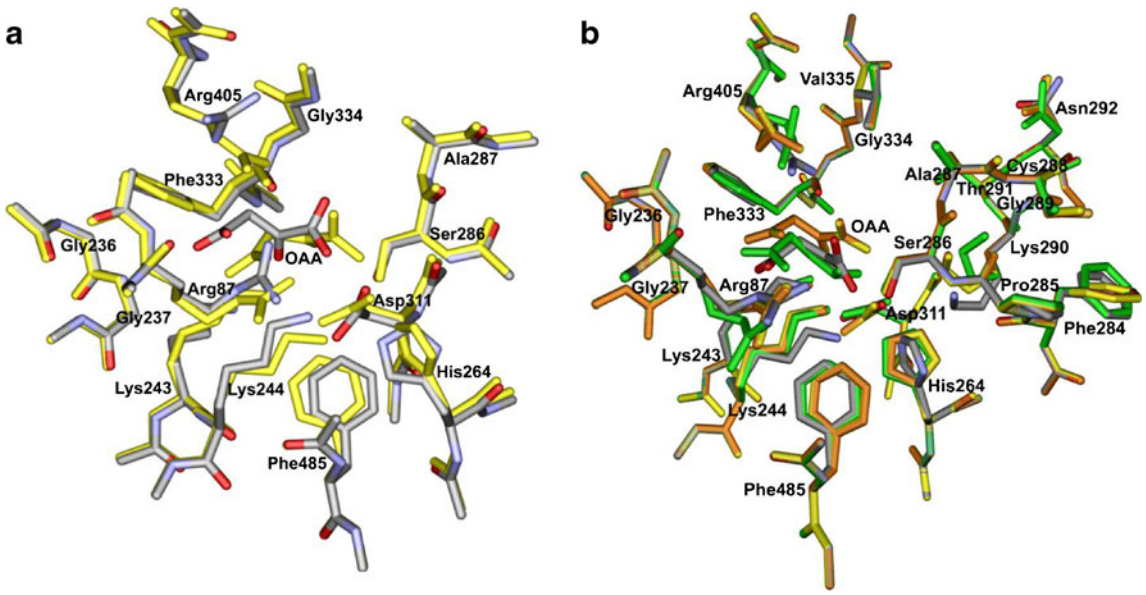

Fig. 2 Backbone superimposition of **a** OAA and 13 residues surrounding the PEPCKnoHS binding pocket obtained from the ONIOM2 (B3LYP/6-31G(d):PM3) method with HAF (*yellow*) and BBF (color by element) approximations and **b** PEPCKnoHS complexes for the X-ray (color by element), B3LYP/6-31G(d):PM3 (*yellow*), B3LYP/6-31G(d):PM3MM (*orange*), and B3LYP/6-31G(d):PM6 (*green*) structures

from the X-ray structure, especially the OAA orientation. These results can be explained by the fact that the PM3MM method still specifies the PM3 model, and includes the optional molecular mechanic correction. Interestingly, the B3LYP/6-31G(d):PM6 method gives the OAA position in the pocket close to that in the crystal structure while other residues are not significantly different from the B3LYP/6-31G(d):PM3 and B3LYP/6-31G(d):PM3MM structures (see Table S1 in Supplementary materials). Moreover, the B3LYP/6-31G(d):PM6 method provides the most stable bound state of OAA to the pocket (BE^{ONIOM} is −18.88 kcal mol^{-1}) and the lowest total energy of the complex ($E^{\mathrm{ONIOM}}_{\mathrm{complex}}$ is −533.44 a.u.) while the BE^{ONIOM} and $E^{\mathrm{ONIOM}}_{\mathrm{complex}}$ values for the B3LYP/6-31G(d):PM3 method are −7.75 kcal mol^{-1} and −532.98 a.u., respectively, and for the B3LYP/6-31G(d):PM3MM method are −7.53 kcal mol^{-1} and −532.96 a.u., respectively (see Table S2 in Supplementary materials). These imply that the outer layer using the PM6 method demonstrates more reliable optimized structure than those of the PM3 and PM3MM methods. Therefore, we select the B3LYP/6-31G(d):PM6 method to further study the PEPCKHS complex.

The predicted structure of PEPCK complexed with hydrazine from the docking process shows that hydrazine bound to PEPCK enzyme at the different binding site of OAA. This implies that hydrazine acts as a noncompetitive inhibitor of PEPCK enzyme by binding at the allosteric site, which is in good agreement with the previous experimental results [8]. The backbone atom superimposition of the optimized PEPCKnoHS and PEPCKHS structures calculated using the ONIOM2 (B3LYP/6-31G(d):PM6) method is displayed in Fig. 3. It clearly demonstrates that after hydrazine bound to the PEPCK complex, the orientation of OAA in the binding pocket is different from the unbound complex. This is due to the conformational change of the pocket after hydrazine included influences directly to the position of OAA. We observed two proton transfers in the PEPCKHS complex. First, the proton was transferred from a carboxylic group of OAA to the N atom of hydrazine in which the shortest heavy atom-to-heavy atom distances between OAA to hydrazine is about 2.70 Å, as presented in Fig. 4b. Second, the proton transfers from Asp311 to Lys244, resulting in the generation of Asp311 (negative chages) and Lys244 (positive charge). Compared with the PEPCKnoHS complex, the OAA-Lys244 distance is greatly increased from 1.65 Å to 4.76 when hydrazine was incorporated, whereas the Lys244-Asp311 is significantly decreased from 3.83 to 2.69 Å (Fig. 4a and b). These imply that hydrazine shortens the Lys244-Asp311 distance and induces the formation of the proton transferring between both residues. Such a process causes the strong interaction between OAA and the PEPCK binding pocket through the electrostatic interaction.

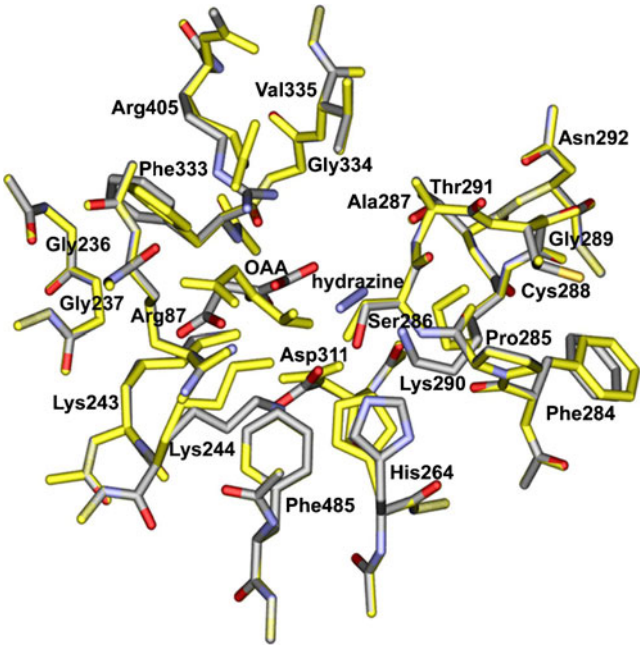

Fig. 3 Backbone superimposition of PEPCKnoHS (*yellow*) and PEPCKHS (color by element) optimized using the ONIOM2 (B3LYP/6-31G(d):PM6) method

Interaction between oxaloacetic/oxaloacetate and individual residues in the PEPCKnoHS and PEPCKHS complexes

As we discussed in the previous section, the conformational changes of some residues in the binding site after hydrazine incorporated to the system result in the change of the interaction between OAA and the pocket and may cause blocking of the reaction. In order to provide an in-depth analysis the particular interactions between OAA and individual residues surrounding the binding pocket of PEPCKnoHS and PEPCKHS were performed by employing the MP2/6-31G(d,p) method. The calculated interaction energies between OAA and individual residues in the PEPCKnoHS and PEPCKHS complexes are listed in Table 1 and graphically presented in Fig. 5. It was found that the total interaction between OAA and all residues for PEPCKnoHS demonstrates the attractive force of −15.68 kcal mol^{-1}. Furthermore, Arg87, Gly237, Ser286, and Arg405 play an important role in the binding to OAA with the interaction energies of −1.93, −2.06, −2.47, and −3.16 kcal mol^{-1}, respectively, which are approximately equal to ~61 % of all interactions. The strong interactions between OAA and the four residues originate from the formation of hydrogen bond interactions, as shown in Fig. 6. The hydrogen bond distances were defined as the length from a heavy atom to an oxygen or nitrogen atom and were observed in the range of ~2 to 3 Å. In the case of Arg405-OAA interaction, we also observed weak hydrogen bonding interactions with the distances of ~4 Å. Other

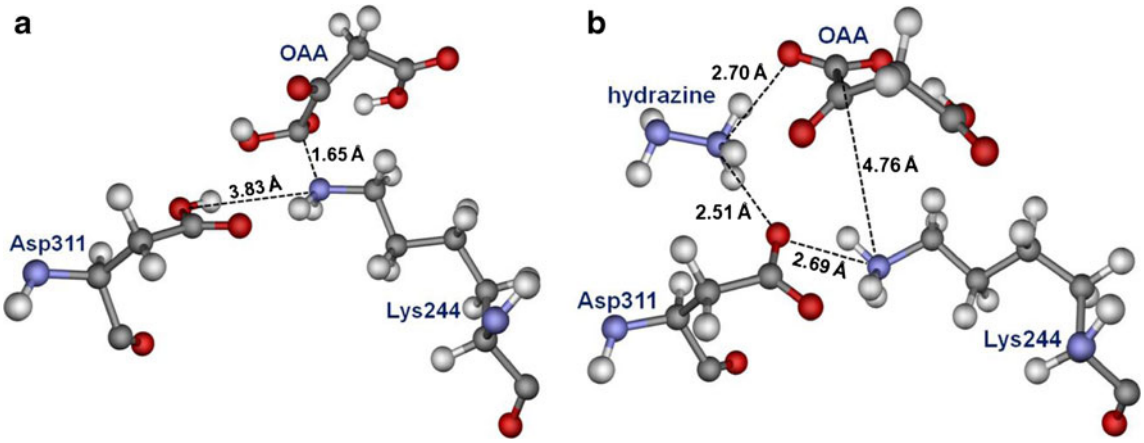

Fig. 4 Intermolecular distances among **a** OAA, Lys244, and Asp 311 in the binding pocket of PEPCKnoHS and **b** OAA (charge −1), hydrazine (charge +1), Lys244 (charge +1), and Asp311 (charge −1) in PEPCKHS. The distances are defined as the nearest length between a heavy atom to a heavy atom of each molecule

residues in the binding pocket demonstrate only van der Waal interactions to OAA, resulting in the presence of low interaction energies less than 1 kcal mol^{-1} except Lys244 (−1.11 kcal mol^{-1}) and Phe333 (−1.45 kcal mol^{-1}).

After hydrazine was included into the PEPCK complex, the total interaction between all residues and OAA becomes more attractive than that found in the PEPCKnoHS complex ~127 % (from −15.68 to −35.61 kcal mol^{-1}). The dramatic increase of the total attraction in PEPCKHS is mainly from the electrostatic attractive force between OAA and Lys244 (*INT* is −70.55 kcal mol^{-1}). However, the great repulsive interaction between OAA and Asp311 (*INT* is 63.65 kcal mol^{-1}) also

Table 1 Interaction energies (*INT*) of OAA and 21 residues surrounding the binding pockets of PEPCKnoHS and PEPCKHS, calculated at MP2/6-31G(d,p) level with BSSE correction, using ONIOM2(B3LYP/6-31G(d):PM6) optimized geometries

Amino residues (X_i)	*INT* (kcal/mol)		Δ*INT*[a] (kcal/mol)
	PEPCKnoHS	PEPCKHS	
Arg87	−1.93	−1.08	0.85
Gly236	−0.65	−0.95	−0.30
Gly237	−2.06	−1.51	0.55
Lys243	−0.81	−6.60	−5.79
Lys244	−1.11	−70.55	−69.45
His264	−0.82	4.37	5.18
Phe284	0.02	1.25	1.23
Pro285	−0.15	0.34	0.49
Ser286	−2.47	−5.40	−2.94
Ala287	−0.06	−3.20	−3.13
Cys288	0.07	−2.18	−2.25
Gly289	0.05	−1.28	−1.13
Lys290	−0.21	1.29	1.50
Thr291	0.01	−0.72	−0.73
Asn292	−0.04	0.57	0.62
Asp311	−0.09	63.65	63.74
Phe333	−1.45	2.36	3.81
Gly334	0.14	−2.72	−2.86
Val335	−0.15	−1.71	−1.57
Arg405	−3.16	−10.35	−7.19
Phe485	−0.82	−1.17	−0.35
Sum	−15.68	−35.61	−19.93
HS		−108.45	

[a] $\Delta INT = INT_{PEPCKHS} - INT_{PEPCKnoHS}$; positive values imply that the binding ability of OAA to residues are decreased after incorporation of hydrazine into the complex

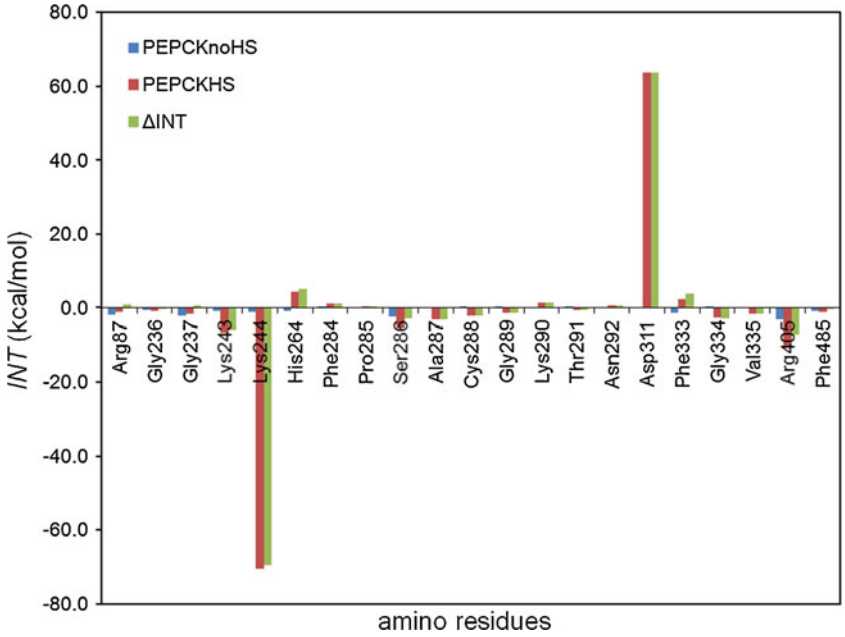

Fig. 5 Interaction energies (*INT*) between OAA and 21 residues surrounding the PEPCK binding pocket in the PEPCKnoHS (*blue bar*), PEPCKHS (*red bar*), and Δ*INT* of PEPCKnoHS and PEPCKHS (*green bar*), calculated using the MP2/6-31G(d,p) method

reduces the binding of OAA and the pocket. We noticed that hydrazine strongly interacts with OAA with the *INT* value of −108.45 kcal mol^{-1}, causing the deviation of the OAA orientation in the pocket. Furthermore, we observed that hydrazine also influences to the orientations of some other residues, especially Lys243, His264, Phe333, and Arg405, in the binding pocket. These residue orientations were slightly deviated compared with those in PEPCKnoHS. In detail, Lys243 and Arg405 move toward OAA, presenting the shorter distances of ~0.2 Å than in PEPCKnoHS. Since the intermolecular interaction between OAA and residues is inversely proportional to the distance between them, Lys243 and Arg405 exhibit an increase of binding strength to OAA with Δ*INT* of −5.79 and −7.19 kcal mol^{-1}, respectively. On the other hand,

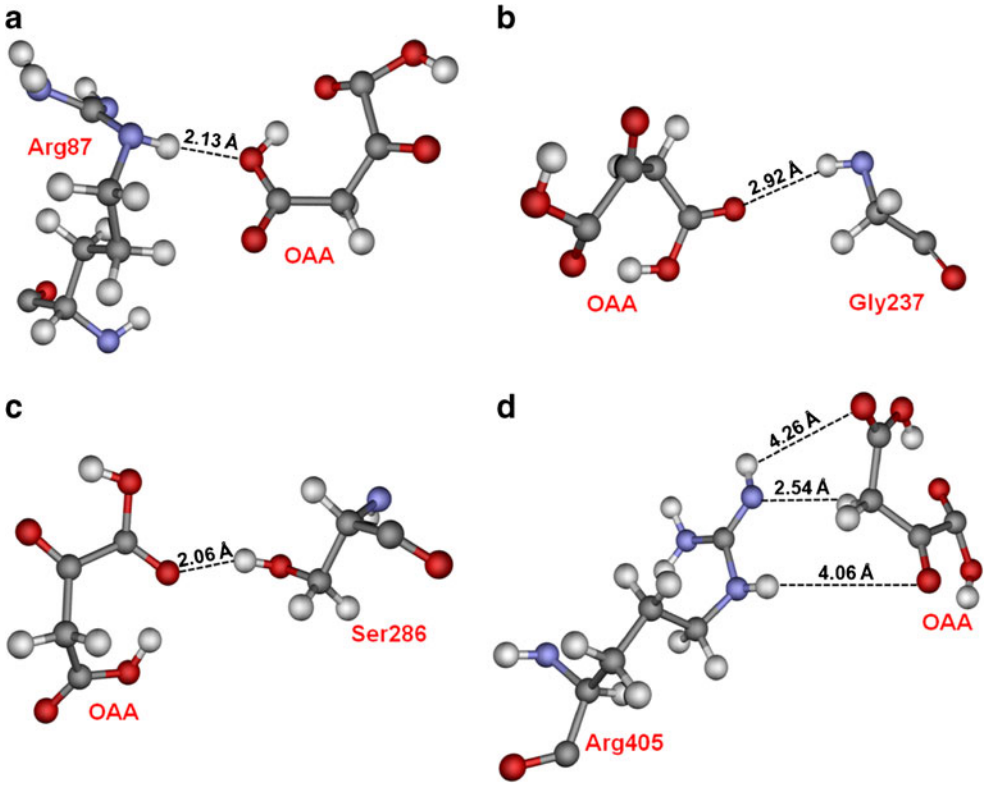

Fig. 6 Hydrogen bonding interaction distances between OAA and **a** Arg87, **b** Gly237, **c** Ser286, and **d** Arg405 in the PEPCKnoHS complex

the distances measured from His264 and Phe333 to OAA in the PEPCKHS complex are longer than ones in PEPCKnoHS by about ~0.2 Å, causing the lower binding to OAA (ΔINT= 5.18 and 3.81 kcal mol^{-1}, respectively). This indicates that hydrazine does not only tightly bind and change the orientation of OAA in the pocket, but also affect directly the binding ability of OAA to the PEPCK binding site by changing the orientation of residues surrounding the pocket. These lead to generate the enzyme-ligand-inhibitor complex which is not appropriate to subsequently form the final product such as PEP. Such knowledge can pave the way to synthesize new hydrazine-based compounds.

Conclusions

The hydrazine blocking of gluconeogenesis process through PEPCK inhibition was performed using quantum chemical calculations based on the ONIOM2 method. The combined B3LYP/6-31G(d) and PM6 was successfully applied and revealed deviation of the orientation and binding strength of OAA to the PEPCK binding pocket after hydrazine incorporated. The computational models were classified into two systems; PEPCK not composing hydrazine inhibitor (PEPCKnoHS) and PEPCK composing hydrazine inhibitor (PEPCKHS). For the former system, Arg87, Gly237, Ser286, and Arg405 play an important role in the binding to OAA through hydrogen bonding interactions. In the case of the latter system, we observed the proton transfer reactions from OAA to hydrazine and Asp311 to Lys244. Such reactions cause a huge increase of the binding strength of OAA to the PEPCK pocket. Comparing both systems, the conformation of the PEPCK binding pockets are partially different, especially Lys243, Lys244, His264, Asp311, Phe333, and Arg405. Moreover, the MP2 calculations indicated that OAA strongly bound to hydrazine, resulting in the significant change of the OAA orientation in the binding pocket. This leads to generate the PEPCK-OAA-HS complex which is not appropriate to subsequently produce phosphoenolpyruvate. Taken into account, understanding of the function of hydrazine inhibitor and key role residues in the binding to OAA might be useful in the design of new hydrazine-based compounds used for antichachexia agents. The designed compounds should hinder the interactions between OAA and key residues, i.e., Arg87, Gly237, Ser286, and Arg405.

Acknowledgments This work is supported by the Thailand Research Fund (RTA5380010). P.P is grateful to the Development and Promotion of Science and Technology Talents (DPST) project for a scholarship and research supporting. We also thank Kasetsart University Research and Development Institute (KURDI), Laboratory of Computational and Applied Chemistry (LCAC), the Commission on Higher Education, Ministry of Education [through the "National Research University Project of Thailand (NRU)" and the "National Center of Excellence for Petroleum, Petrochemical and Advanced Materials (NCEPPAM)"] for research facilities. The Large Scale Simulation Research at NECTEC is gratefully acknowledged for SYBYL software and computing resources. We also thank to Dr. Patchreenart Saparpakorn for helpful discussion.

References

1. Kaegi E (1998) CMAJ 158:1327–1330
2. Ernst E, Cassileth BR (1999) Eur J Cancer 35:1608–1613
3. Pfeiffer N (1991) Oncol Times 12:14
4. Gold J (1974) Oncology 29:74–89
5. Gold J (1975) Oncology 32:1–10
6. Gold J (1981) Nutr Cancer 3:13–19
7. Gold J (1987) Nutr Cancer 9:59–66
8. Ray PD, Hanson RL, Lardy HA (1970) J Biol Chem 245:690–696
9. Silverstein R, Bhatia P, Svoboda DJ (1989) Immunopharmacol 17:37–43
10. Mazzio E, Soliman KFA (2003) Neurotoxicology 24:137–147
11. Hughes TK, Cadet P, Larned CS (1989) Int J Immunopharmacol 11:501–507
12. Bruera E (1992) Oncology 6:125–130
13. Jia F, Morrison DC, Silverstein R (1994) Circ Shock 42:111–114
14. Toth B (1972) Int J Canc 9:109–118
15. Hainer MI, Tsai N, Komura ST, Chiu CL (2000) Ann Intern Med 133:877–880
16. Luyckx VA (2012) Adv Chron Kid Dis 19:129–141
17. Ravoof TBSA, Crouse KA, Tahir MIM, How FNF, Rosli R, Watkins DJ (2010) Transit Metal Chem 35:871–876
18. Baumann RP, Penketh PG, Ishiguro K, Shyam K, Zhu YL, Sartorelli AC (2010) Biochem Pharmacol 79:1553–1561
19. Baumann RP, Ishiguro K, Penketh PG, Shyam K, Zhu R, Sartorelli AC (2011) Biochem Pharmacol 81:1201–1210
20. De P, Baltas M, Lamoral-Theys D, Bruyere C, Kiss R, Bedos-Belval F, Saffon N (2010) Bioorg Med Chem 18:2537–2548
21. Kakadiya R, Dong H, Kumar A, Narsinh D, Zhang X, Chou T-C, Lee T-C, Shah A, Su T-L (2010) Bioorg Med Chem 18:2285–2299
22. Grande F, Yamada R, Cao X, Aiello F, Garofalo A, Neamati N (2009) Expert Opin Investig Drugs 18:555–568
23. Zheng L-W, Wu L-L, Zhao B-X, Dong W-L, Miao J-Y (2009) Bioorg Med Chem 17:1957–1962
24. Passarella S, Palmieri F, Quagliariello E (1977) Arch Biochem Biophys 180:160–168
25. Scrutton MC (1978) FEBS Lett 89:1–9
26. Darvey IG (2000) Biochem Educ 28:80–82
27. Llanos L, Briones R, Yévenes A, González-Nilo FD, Frey PA, Cardemil E (2001) FEBS Lett 493:1–5
28. Morokuma K (2002) Philos Transact A Math Phys Eng Sci 360:1149–1164
29. Kitisripanya N, Saparpakorn P, Wolschann P, Hannongbua S (2011) Nanomed-Nanotechnol 7:60–68
30. Boonsri P, Kuno M, Hannongbua S (2011) Med Chem Comm 2:1181–1187
31. Srivab P, Hannongbua S (2008) ChemMedChem 3:803–811
32. Kuno M, Hongkrengkai R, Hannongbua S (2006) Chem Phys Lett 424:172–177
33. Saen-Oon S, Kuno H, Hannongbua S (2005) Proteins 61:859–869
34. Nunrium P, Kuno M, Saen-Oon S, Hannongbua S (2005) Chem Phys Lett 405:198–202
35. Sae-Tang D, Kittakoop P, Hannongbua S (2009) Monatsh Chem 140:1533–1541

36. Maitarad P, Kamchonwongpaisan S, Vanichtanankul J, Vilaivan T, Yuthavong Y, Hannongbua SJ (2009) Comput Aided Mol Des 23(4):241–252
37. Alzate-Morales JH, Caballero J, Gonzalez-Nilo FD, Contreras R (2009) Chem Phys Lett 479:149–155
38. Kuno M, Hannongbua S, Morokuma K (2003) Chem Phys Lett 380:456–463
39. Sullivan SM, Holyoak T (2007) Biochem 46:10078–10088
40. Tripos Associates. SYBYL7.2. St. Louis, MO: Tripos Associates Inc (2006)
41. Frisch MJ, Trucks GW, Schlegel HB et al. (2009) Gaussian 09, Revision A1. Gaussian, Inc, Wallingford
42. Morris GM, Goodsell DS, Halliday RS, Huey R, Hart WE, Belew RK, Olson AJ (1998) J Comput Chem 19:1639–1662
43. Benjahad A, Guillemont J, Andries K, Nguyen CH, Grierson DS (2005) J Med Chem 48:1948–1964